ADVANCED ENGINEERING MATERIALS

DOI: 10.1002/adem.200700009

ESR Refining Potential for Titanium Alloys using a CaF_2-based Active Slag**

By *J.-C. Stoephasius, J. Reitz* and *B. Friedrich*

Since the end of the Cold War and due to the needs to produce titanium more cost-efficient and thus more attractive for its civilian use, the electroslag remelting (ESR) process has become an increasingly important topic of international research programmes, because titanium and titanium aluminides can be chemically refined by ESR in some degree. Using ESR, titanium turnings from machining steps and scrap from foundries can be remelted, refined and provided as secondary titanium for the market at relatively favourable prices. This article investigates the removability of the main impurities out of titanium and titanium-aluminium alloys by electroslag remelting using the active slag system CaF_2-Ca-(CaO). Thermochemical and kinetic aspects of the ESR process are considered.

1. Introduction

Already in the 1930s a forerunner of the ESR based on direct current slag melting was developed by R. K. Hopkins, USA. In 1957 the first industrial alternating current furnace for the remelting of titanium was put in operation in the USSR. Since the 1970s, however, vacuum arc remelting (VAR) has replaced the ESR for the remelting of titanium, even though for no obvious reasons. But since the end of the Cold War and due to the needs to produce titanium more cost-efficient and thus more attractive for its civilian use, the ESR process has become an increasingly important topic of international research programmes.[1]

Contrary to the VAR process, titanium can be chemically refined by ESR in some degree as shown before.[2,3,4,5] Using ESR titanium turnings from machining steps and scrap from foundries can be remelted, refined and provided as secondary titanium for the market at relatively favourable prices. This article investigates the thermochemical equilibria of oxygen, nitrogen, hydrogen, fluorine and calcium with titanium and titanium aluminides using the active slag system CaF_2-Ca-(CaO). It's shown, that the oxygen content in titanium and titanium alloys can be reduced by electroslag remelting with a metallic Ca-containing CaF_2 slag to values, conforming to material standards. Hydrogen is also almost completely removed by remelting. Dissolved nitrogen cannot be removed, but is nevertheless homogeneously distributed. The demanded contents of less than 300 ppm are assured even after multiple remelting steps. In a small quantity titanium and ti-

[*] **Please check title and addresses of authors!**
J.-C. Stoephasius, J. Reitz, Prof. B. Friedrich
IME Process Metallurgy and Metal Recycling
Department and Chair of RWTH Aachen University
E-mail: JStoephasius@ime-aachen.de

[**] *The authors would like to acknowledge the Arbeitsgemeinschaft industrieller Forschungsvereinigungen "Otto von Guericke" e.V. (AiF)(contract No. 14030 N) for support of the development of the IME-γ-TiAl-process with funds from the Bundesministerium für Wirtschaft und Arbeit (BMWA), the German Research Foundation (DFG)(contract No. FR 1713/2-1) for support of the research in electroslag remelting fundamentals, and the DLR Deutsches Zentrum für Luft- und Raumfahrt e.V. (contract No. BMBF 01 RW 0410) for support of the development of a process for titanium recycling in an electroslag remelting furnace with funds from the Bundesministerium für Bildung und Forschung (BMBF).*

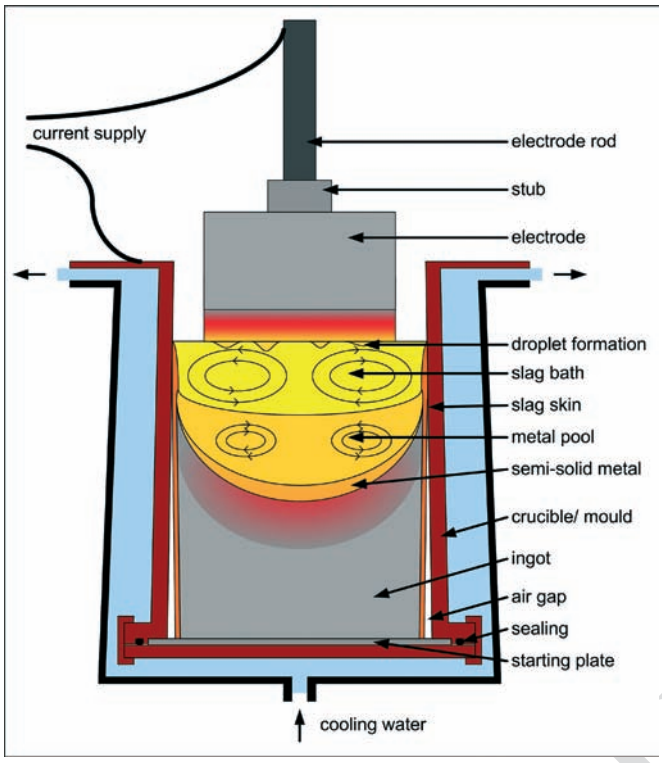

Fig. 1. Principle of the electroslag remelting process.

tanium alloys absorb fluorine and calcium from the slag. Examinations of test specimens will have to show the effects of these impurities on the material properties.

2. Basic Principles of Electroslag Remelting

The basic mechanism of ESR is shown in Figure 1. The procedure utilises the fact that as an ionic conductor slag has a considerably higher resistance than metals (electronic conductors) even at higher temperatures. An electrical current flows through an electrode rod, a stub, welded to an electrode, and the electrode itself into a slag bath. The current leaves the system through the liquid metal pool at its bottom, the solidified ingot, the bottom plate of the mould and the mould itself (as shown in Fig. 1) or coaxial mounted power bars. The current partly flows directly through a thin solidified slag skin between slag-bath and mould. The necessary voltage of 30–35 V for titanium almost completely drops off in the slag-bath, where hence almost the complete electric power is converted into heat. On the contact surface between the slag and the water-cooled copper mould the above mentioned thin slag skin of a thickness between 1 and 2 mm is formed. This reduces the heat loss and, consequently, the cooling rate of the ingot, thus influencing the solidification structure. The protection of the molten metal bath from direct contact to the copper surface prevents a too fast and inhomogeneous solidification and results in a high surface quality.

Comparatively little heat transport takes place through the electrode, especially in case of metals with low heat conductivity. Thus, when the liquidus temperature is reached, small droplets form on the bottom side. These droplets fall through the slag bath due to their higher density and accumulate in the molten metal bath. Already in the partial liquid state under the electrode, but in particular during the retention time in the molten metal bath the desired refining reactions with the slag take place. Under sloped radial heat dissipation the ingot solidifies directionally. Due to the shrinkage of the ingot during the cooling a stripping of the slag skin from the mould and the formation of an "air"-gap, impeding a further cooling, can be observed. By the natural convection of the slag due to the temperature profile and the effect of the electromagnetic field, vortices form within the slag and the molten metal bath. At too turbulent conditions small slag droplets can be carried away by the metal and incorporated into the ingot. Therefore, a high turbulence in the ESR process is, in contrast to other processes, e. g. vacuum induction melting (VIM), not desired. To avoid a too intense movement of the bath, besides coaxially arranged electric power bars or cables preferably low frequencies of e. g. 2–5 Hz are used.

3. Refining Potential for γ-Titanium Aluminides and Titanium

3.1. Calcium-Oxygen Equilibrium in the Metal

Even actual thermochemical databases as implemented in FactSage 5.4.1 or Thermocalc don't contain appropriate information about the Ca-Ti-O interactions. Therefore, experimental data from Tsukihashi et al.[6] concerning the calcium and oxygen intake by titanium and titanium aluminides were used to calculate the interaction parameters of the following equilibrium reaction:

$$[Ca]_{TiAl} + [TiO]_{TiAl} = [CaO]_{slag} + [Ti]_{TiAl} \quad (1)$$

(where $[A]_B$ means: A is dissolved in B)

Figure 2 shows that this reaction is causal for the equilibrium between calcium and oxygen in titanium and titanium aluminides. It can be seen that the equilibrium constant is

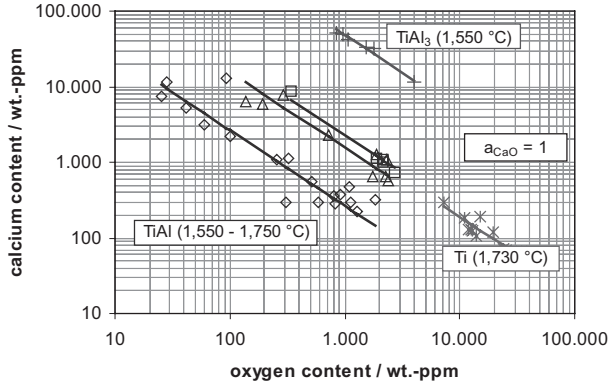

Fig. 2. Dependency of the calcium content in titanium and titanium aluminides from the oxygen content in equilibrium with a CaO-crucible, data.[2]

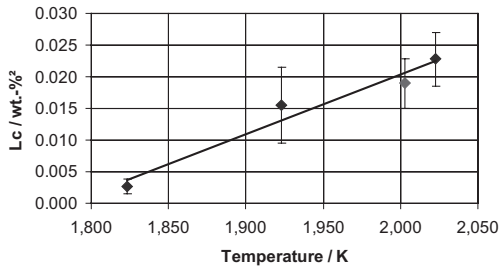

Fig. 3. Solubility product Lc of calcium and oxygen in titanium and TiAl, data.[2]

nearly independent from the composition, but depends strongly on the temperature. It's obvious that titanium and TiAl have the same equilibrium constant, while $TiAl_3$ has about 180 times higher calcium contents at the same oxygen content. This is due to the formation of the intermetallic $CaAl_2$ phase. The Gibbs energy difference between the formation of $CaAl_2$ from TiAl and the formation of $CaAl_2$ from $TiAl_3$ is 79.7 $^{kJ}/_{mole}$ at 1,550 °C which means a factor 192 in the equilibrium constant and is very close to the experimental result. Figure 3 shows that the solubility product of calcium and oxygen in titanium and TiAl can be approximated linearly between 1,550 °C and 1,750 °C. The error bars results from the statistical deviation of the single experiments.

The above presented results don't allow the prediction of the reachable oxygen contents in titanium and titanium aluminides during electroslag remelting, because the calcium partial pressure in the atmosphere wasn't measured and therefore, the distribution coefficient between calcium in the metal and calcium in the slag at known calcium activity in the slag is still unknown. Extending the attempt from Tsukihashi, Okabe et al.[7] adjusted fixed CaO and Ca activities at the same time by adding metallic calcium as third phase. Based on this results the activity coefficient f_{TiO} of TiO in titanium could be calculated and approximated by a simple equation (Eq. 2). The result is in general accordance with the Ti-O interaction in the model of the ternary Al-Ti-O system from Lee and Saunders.[8]

$$f_{TiO} = 6 \cdot 10^{-13} \cdot T^{3.8} \quad T = 1{,}173 \ldots 1{,}573\ K \tag{2}$$

Considering the solubility equilibrium from Figure 2, the calcium intake is 430 ppm and the oxygen intake is 4,400 ppm, if c. p. titanium is equilibrated with pure calcium and calcium oxide ($a_{Ca\ =\ 1}$; $a_{CaO\ =\ 1}$) at 1,730 °C. Under the same conditions, TiAl dissolves 5,300 ppm calcium and 440 ppm oxygen, while at a lower temperature (1,550 °C) but comparable superheat only 3,000 ppm calcium and 90 ppm oxygen are picked up. During electroslag remelting instead of pure CaO a CaF_2-CaO slag is used. Therefore, due to the decreased CaO activity, in general it's possible to deoxidise c. p. titanium below 2,000 ppm oxygen. Suzuki and Inoue[9] introduce following coefficient r as proportional factor for the reachable oxygen contents:

$$r \equiv \frac{a_{CaO,slag}}{a_{Ca,slag}} \tag{3}$$

3.2. Removability of Oxygen during Electroslag Remelting

One of the most challenging tasks in the refining process of titanium alloys is the removal of oxygen present in titanium as dissolved TiO. Besides the high stability of TiO ($\Delta G_F = -513{,}3\ ^{kJ}/_{mole}$) also the oxygen solubility of up to 33 at.-% in the system Ti-O indicates that the removal is difficult. The deoxidation in a VAR or an electron beam furnace (EBF) is not feasible due to the necessary oxygen partial pressure in the furnace atmosphere ($p_O < 3 \cdot 10^{-19}$ bar) which is so low, that even oxygen is nearly fully dissociated. Contrary in the ESR the high oxygen affinity of a CaF_2-slag containing Ca offers a sufficient deoxidation potential as shown in the previous chapter. During the deoxidation process a large amount of CaO is formed and therefore, slag composition and CaO activity change significantly. In order to achieve constant oxygen contents, the r-factor must be held constant by increasing the calcium concentration in the slag. Therefore, the activity coefficients of the ternary CaF_2-Ca-CaO slag system must be well known in a wide range.

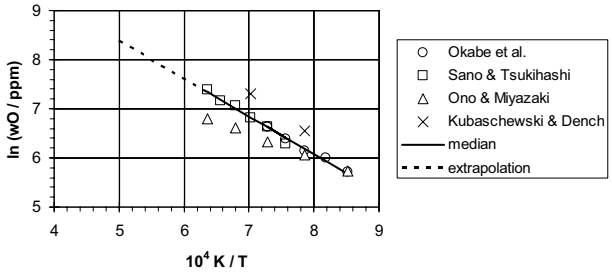

Fig. 4. Temperature dependency of the oxygen content in c. p. titanium in equilibrium with calcium and calcium oxide, data:[3]

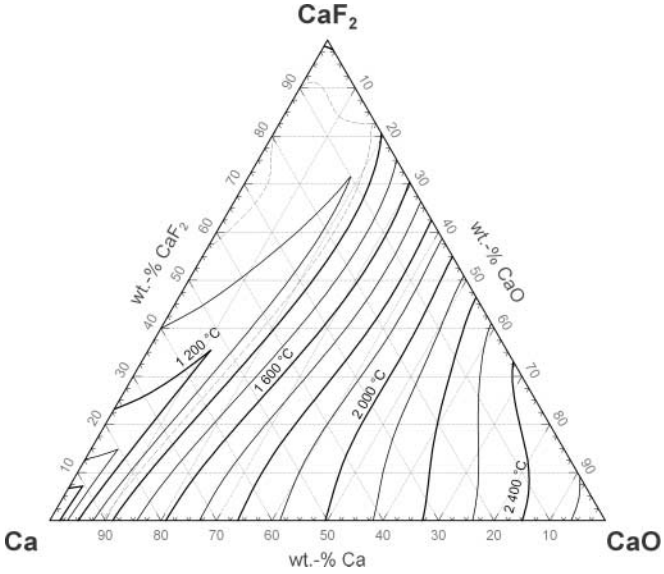

Fig. 5. Calculated CaF_2-Ca-CaO phase diagram, calculation based on the accepted binary subsystems[6–9]

The ternary CaF_2-Ca-CaO slag system was modelled in this work using the FactSage OptiSage module. A Kohler/Toop sublattice type was chosen, since neither special first order relations (e. g. silica fuses: quasi chemical model) nor a special alloying trend (metallic melts: compound energy formalism) was estimated. Due to the higher precision at the boundaries the Kohler/Toop algorithm was preferred to the Muggianu algorithm. As data basis for the model the eutectic points and some of the liquidus lines of the accepted binary systems Ca-CaF_2,[10–12] Ca-CaO[12] and CaF_2-CaO[13] were taken. The calculated CaF_2-Ca-CaO phase diagram is shown in Figure 5. The result of this calculation is, that the calcium content in the slag must be adjusted in accordance to Figure 6, in order to achieve specification conform oxygen levels in titanium and TiAl, respectively during the process. Because of the high vapour pressure of calcium, in general only low calcium contents in the slag can be processed. Therefore, c. p. titanium can be deoxidised only at low CaO contents in the slag and the deoxidation capacity of the slag is rather low. Contrary titanium aluminides can be deoxidised over the whole range of acceptable CaO contents.

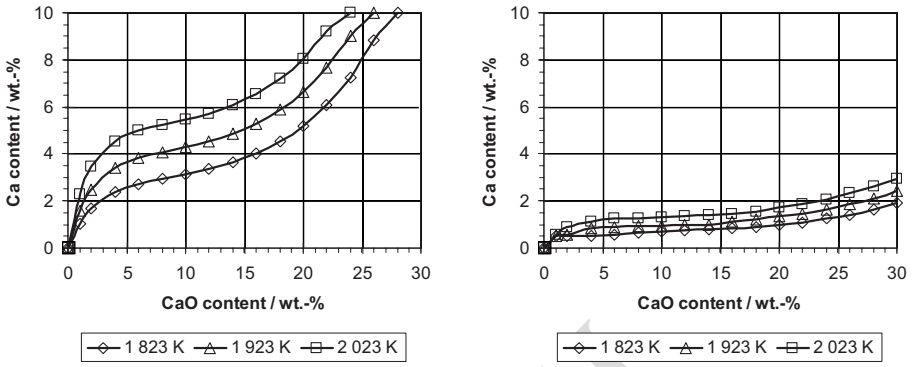

Fig. 6. Necessary Ca content in the slag in order to achieve specification conform oxygen contents in titanium (left: r = 0.4) and titanium aluminide (right: r = 2).

3.3. Removability of Nitrogen

Titanium nitride ranks among the most stable nitride compounds present in metallurgy. Only from the stoichiometric reaction with the very unnoble elements Zr and Th result even more negative free enthalpy values for their nitride formation (table 1). Thus a chemical refining of nitrogen containing titanium electrodes or titanium aluminide electrodes is to be ruled out. Since the density of titanium nitride is with 5430 $^{kg}/_{m^3}$ higher than that of the metal phase and the liquidus temperature ranges between 2350 and 3290 °C, also physical processes for the separation of undissolved nitrides, such as evaporation or flotation, can be excluded.

Concerning nitrogen impurities only a structural refining by homogenisation can be achieved using electroslag remelting. Benz and Carter[14] describe the possibility of removing nitrogenous inclusions from titanium sponge. They state, that even very large titanium nitride inclusions (φ 10 × 10 mm) can be dissolved in a CaF_2-slag containing calcium. They propose that nitrogen, which is dissolved in the slag, remigrates to the electrode, is absorbed from the droplet phase boundary and homogeneously dissolved from the metal. Scholz et al.[15] have shown that during ESR of titanium using a technical pure CaF_2-slag the nitrogen content on average increases from 120 to 150 ppm. This indicates, that there is no significant nitrogen solubility in calcium fluoride which would lead to decreasing nitrogen contents in the metal. This result is in accordance with examinations from Ryabtsev et al.[16, 17] who proofed, that removing of nitrogen rich inclusions (NRI) is practically impossible using a pure CaF_2-slag. This is due to the very low dissolution rate (diffusion-controlled). Contrary to that the removing is successful at high remelting rates using Ca-containing active slags due to the low nitrogen activity in the slag and gas phase. Ryabtsev observed as well,[16] that nitrogen can be transferred into the gas phase since evaporated calcium reduces the nitrogen partial pressure below 10^{-15} bar.

Own examinations also showed, that only at very low solidification rates thin titanium nitride inclusions can be dis-

Table 1. Gibbs free enthalpy of the stoichiometric reaction of TiN with various metals.

metal	$\Delta G°_R$ [$^J/_{mole\ N}$]			compound	metal	$\Delta G°_R$ [$^J/_{mole\ N}$]			compound
	1,600 °C	1,700 °C	1,800 °C			1,600 °C	1,700 °C	1,800 °C	
Si	358,000	342,300	325,600	SiN	La	64,600	66,100	67,100	LaN
$1^1/_2$ Mg	340,000	332,500	324,600	$^1/_2\ Mg_3N_2$	Al	51,500	53,700	55,400	AlN
Ba	210,200	212,300	213,800	BaN	Y	50,500	51,800	52,600	YN
$1^1/_2$ Ca	145,200	158,400	171,000	$^1/_2\ Ca_3N_2$	Zr	-29,200	-29,600	-30,600	ZrN
B	74,000	73,100	71,700	BN	Th	-53,800	-54,700	-55,700	ThN

Fig. 7. Formation of TiN in aluminothermic TiAl at the broken electrode surface using a copper mould (electrode head).

solved by diffusion. In γ-titanium-aluminide castings after aluminothermic reduction the residual nitrogen in the mould forms titanium nitrides (Fig. 7). Such inclusions often lead to the fracture of the electrode. This effect has only been observed at high cooling rates, if a water-cooled copper mould was used. At a slow cooling rate using a ceramic mould, nitrogen from the titanium nitrides was dissolved homogeneously in the surrounding titanium-aluminide matrix.

3.4. Removability of Hydrogen

Alvarez et al.[18] have proved a considerable decrease of the ductility of pure titanium for hydrogen contents above 3,5 at.-%. Chen et al.[19] have also shown that in pure titanium which was equilibrated at 400 °C already at 77 ppm γ-titanium-hydrides and at 350 ppm δ-titanium-hydrides occur. However, due to the similar crystal structure and their small size (< 400 nm), these hydrides do not significantly influence the plastic deformability. Cracks parallel to the direction of the force appeared during forging only at the hydrogen richest sample (720 ppm hydrogen). Both pure titanium- and γ-titanium-aluminide alloys show a high hydrogen solubility at temperatures below 500 °C. During mechanically alloying of various titanium-aluminium alloys under hydrogen atmosphere Takasaki et al.[20] have obtained hydrogen contents of above 4,670 ppm, but at the same time they could prove the almost complete removability of hydrogen already at temperatures of 530 °C for Ti_3Al, Ti_2Al and TiAl.

If during cooling of ESR-ingots the presence of hydrogen is avoided in the critical range between 300 and 500 °C, contents of < 100 ppm (ASTM, billets, Grade 1) and < 130 ppm (DIN standard, semifinished products, Grade 1), respectively can be observed. In laboratory tests of ALD Vacuum Technologies[15] even 25 ± 10 ppm have been achieved. It was always possible to reduce the hydrogen content of the electrode by electroslag remelting independent of the initial hydrogen content (25–100 ppm).

Fluorine Absorption of the Metal from CaF_2-Containing ESR-Slags

Scholz et al.[15] experimentally proved that a small fluorine pick up of c. p. titanium is unavoidable during remelting with a standard ESR slag. The measured fluorine content of 60 ppm can already be comprehended by a simple thermochemical calculation: Scholz et al. used a technically pure CaF_2-slag. At process temperatures CaF_2 decomposes to a limited degree, and hence according to Equations 4 and 5 the titanium melt will accumulate fluorine. Assuming ideal conditions, an equilibrium fluorine content of 100 ppm results for the liquid metal according to Equation 6. Considering kinetic inhibitions and the influence of small amounts of CaO which decreases the CaF_2 decomposition, these thermochemical calculations are in good accordance with the experimental results.

$$(CaF_2) = \{CaF\} + \{F\} \quad | \ \Delta G°_{R\_1,873 - 2,173\ K} = 932{,}920 - 241.2 \cdot T\ [^{J}/_{mole}] \tag{4}$$

$$(Ti) + \{F\} = [TiF]_{Ti} \quad | \ \Delta G°_{R\_1,873 - 2,173\ K} = -183{,}380 - 16.75 \cdot T\ [^{J}/_{mole}] \tag{5}$$

$$w_F \approx \frac{M_F}{M_{Ti}} \cdot \frac{p_F}{p°} = \frac{M_F}{M_{Ti}} \cdot \sqrt{k \cdot a_{CaF2} \cdot a_{Ti}} = \frac{M_F}{M_{Ti}} \cdot e^{-\frac{\Delta G^0_{ges}}{2RT}} \tag{6}$$

(w_F: fluorine content in titanium [10^{-6} ppm]; ΔG: Gibbs free reaction enthalpy [J/mole]; k: equilibrium constant [1]; R: ideal gas constant [8.314 J/kgK]; T: temperature [K]; a_i: activity of the component i [1]; p_F: fluorine partial pressure [Pa]; p^0: reference pressure [101,325 Pa]; M_i: molar mass of the substance i [kg/mole])

Contrary to the c. p. titanium experiment it's impossible to calculate the fluorine contents in γ-TiAl exactly due to insufficient thermochemical data of the Ti-Al-F system. But the equilibrium fluorine contents of γ-TiAl should be considerably lower than of pure titanium, since first the process temperature is only approx. 1,600 °C (such the fluorine partial pressure in the furnace atmosphere is by factor 25 smaller) and second, the titanium activity in titanium aluminides is only about 0.25. A third aspect is, that during the deoxidation process a Ca-containing slag is used. The activity of Ca in such a slag is significantly higher than in pure CaF_2. Therefore, Reaction 7 takes place. According to the law of mass action the fluorine partial pressure is thus further reduced (Fig. 8).

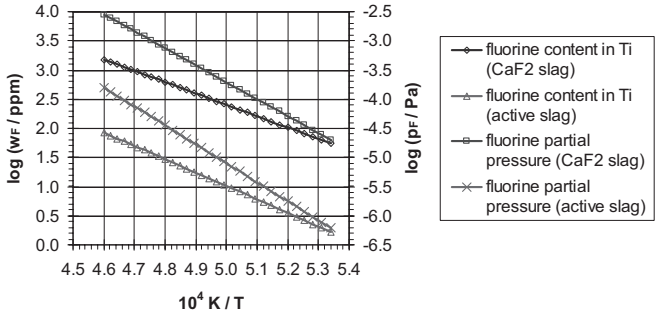

Fig. 8. Fluorine content w_F in c. p. titanium and fluorine partial pressure p_F using a standard and an active (0.5 wt.-% Ca) CaF_2 slag.

$$\{Ca\} + \{F\} = \{CaF\} \quad | \Delta G°_{R\_1,873-2,173\ K} = -183,380 - 16.75 \cdot T\ [^{J}/_{mole}] \tag{7}$$

3.6. Evaporation Losses of Ca

At a typical process temperature of 1,750 °C the partial pressure of calcium in the slag reaches almost 0.5 bar (w_{Ca} = 3 wt.-%). This indicates that high evaporation losses of calcium must be assumed. But the forecast of the evaporation losses of calcium from the slag by purely thermochemical equilibrium states is ineligible without considering the kinetic influencing factors. Figure 9 shows, that there are in general three evaporation steps which can control the overall evaporation rate. At both sides of the slag-gas-boundary there is a diffusion controlled layer, which thickness is influenced from the turbulence in slag and gas phase, respectively. In both diffusion layers the (virtual) calcium partial pressure is reduced according to a diffusion coefficient and the thickness of the diffusion layer. Generally, the evaporation rate of a substance i from a melt is described according to Hertz-Knudson as seen in Equation 8. The coefficients α_V und α_K reflect the fraction of the particle collisions that virtually leads to an evaporation and condensation, respectively. In this particular case they can be estimated to 1.

$$j = j_V - j_K = \alpha_V \cdot \frac{1}{\sqrt{2\pi M_i R T}} \cdot p_{i,S,G} - \alpha_K \cdot \frac{1}{\sqrt{2\pi M_i R T}} \cdot p_{i,G,G} \tag{8}$$

(j: evaporation rate [mole/m^{2}s]; j_V: evaporation stream [mole/m^{2}s]; j_K: condensation stream [mole/m^{2}s]; α_V: evaporation coefficient [1]; α_K: condensation coefficient [1]; M_i: molar mass of the substance i [kg/mole]; R: ideal gas constant [8.314 J/kgK]; T: temperature [K]; $p_{i,S,G}$: partial pressure of the substance i in the melt at the phase boundary [Pa]; $p_{i,G,G}$: partial pressure of the substance i in the gaseous phase at the phase boundary [mole/m^3])

The evaporation step according to Hertz-Knudsen is extremely fast (1,130 $^{mole}/_{m^2 s}$ at 1,700 °C), if an unlimited calcium transport in the gaseous phase is assumed. Therefore, the evaporation itself doesn't seem to be the limiting step for the calcium losses. While the partial pressure of calcium in the slag is not pressure-dependent, the system pressure in the PESR chamber influences the calcium evaporation rate. This is due to the fact that the partial pressure in the gaseous phase at the phase boundary increases and thus the condensation stream is raised. Therefore, the material transport in the gaseous phase must be assumed to be the evaporation limiting step. The calcium transport through the diffusion layer in the gaseous phase is described by the 1st Fick's law (Eq. 9). Assuming, that neither the diffusion in the melt nor the evaporation step are limiting, $p_{Ca,G,G}$ is nearly equal to $p_{Ca,S}$. The diffusion coefficient can be calculated rather easily from the kinetic gas theory and the medium free length of movement without collision according to Equation 10.

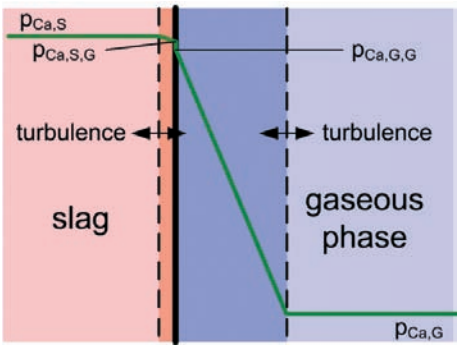

Fig. 9. General model of the transport steps during the evaporation of calcium ($p_{Ca,S}$: virtual partial pressure of calcium in the slag; $p_{Ca,S,G}$: virtual partial pressure of calcium in the slag at the phase boundary; $p_{Ca,G,G}$: partial pressure of calcium in the gaseous phase at the phase boundary; $p_{Ca,G}$: partial pressure of calcium in the gaseous phase).

Figure 10. PESR/ ESR pilot scale furnace at IME Aachen.

$$j = -D \cdot \frac{\Delta c}{\Delta x} = -\frac{D}{\Delta x} \cdot \frac{p_{Ca,G,G}}{R T} \approx -\frac{D}{\Delta x} \cdot \frac{p_{Ca,S}}{R T} \tag{9}$$

(D: diffusion coefficient [m^2/s]; Δc: concentration difference [mole/m^3]; Δx: thickness of the diffusion layer [m])

$$D = \frac{3}{16} v \lambda = \frac{3}{16} \sqrt{\frac{8 R T_S}{\pi \mu_{Ca-Ar}}} \cdot \frac{k T_S}{\sqrt{2} \sigma p} = \frac{3}{8} \sqrt{\frac{k^2 R T_S^3}{\pi \mu_{Ca-Ar} \sigma^2 p^2}} \sim \frac{1}{p} \tag{10}$$

(D: diffusion coefficient [m^2/s]; $\sqrt{V}$: average velocity [m/s]; λ: medium free length of movement without collision [m]; k: Boltzmann's constant [1.38·10^{-23} J/K]; R: ideal gas constant [8.314 J/kgK]; T_S: temperature at the slag surface [K]; $\mu_{Ca\text{-}Ar}$: reduced molar mass between calcium and argon [kg/mole]; σ: cross section [m^2]; p: total gas pressure [Pa])

The thickness of the diffusion layer is often assumed to be 1 mm, if natural convection occurs and no better information are available. Considering the equivalency of heat and mass transfer a formula was developed, that calculates the thickness as function of the Sherwood Number, which is the equivalency to the well known Nusselt Number (Eq. 11).

$$\Delta x = \frac{L}{Sh} = \frac{L}{0,15 \cdot \sqrt[3]{Gr \cdot Sc \cdot f_2(Sc)}} = \frac{1}{0,15 \cdot \sqrt[3]{\frac{T_S - T_m}{T_m} \cdot \frac{g}{\nu \cdot D_m} \cdot f_2(Sc)}} \sim \frac{1}{p^{2/3}} \quad (11)$$

(L: characteristic length [m]; Sh: Sherwood Number [1]; Gr: Grasshoff Number [1]; Sc: Schmidt Number [1]; f_2(Sc): correction coefficient between viscosity and diffusion [1]; T_m: medium temperature in the gaseous phase [K]; ν: cinematic viscosity [m^2/s]; D_m: diffusion coefficient in the gaseous phase [m^2/s])

The calculation of the evaporation losses according to this model was validated with experiments using a 5 wt.-% Ca-containing CaF_2-slag and steel electrodes (φ 100 mm × 1,000 mm) at total chamber pressures between 2 and 40 bar. The experiments were conducted in the IME pilot scale PESR/ESR furnace (Fig. 10). Slag skin samples were taken along the whole ingot. The amount of evaporated calcium could be calculated from the calcium analysis of the slag skin samples and the total slag amount. Considering the local melt rate, it was possible to calculate the process time in which the slag skin solidified and herewith the evaporation rate of the calcium. Considering the difficulties in sampling and analysing the content of metallic calcium in the slag skin, a very good accordance was received (Fig. 11). The increasing calcium content at the end of the experiments can be explained with the solution of calcium dust which was condensed on the crucible walls from the calcium vapour during the process.

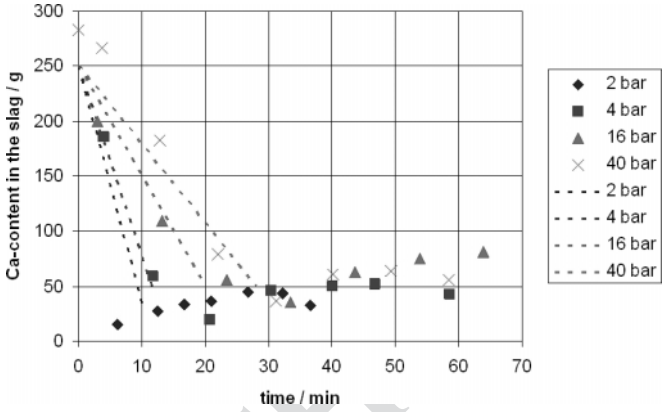

Figure 11. Experimental (points) and theoretical (dashed lines) evaporation of calcium.

4. Conclusion

It has been demonstrated in this article that the oxygen content in titanium and titanium alloys can be reduced by electroslag remelting with a Ca-containing CaF_2-slag to levels, conforming to material standards, below 2,000 ppm (Ti) or 500 ppm (γ-TiAl). Hydrogen too is almost completely removed by remelting (< 35 ppm). Dissolved nitrogen cannot be removed, but is nevertheless homogeneously distributed. The demanded contents of less than 300 ppm are assured even after multiple remelting steps. Titanium and titanium alloys dissolve less than 20 ppm fluorine and up to 50 ppm calcium from the slag. Contrary titanium aluminides dissolve one order of magnitude less fluorine but one order of magnitude more calcium. Examinations of test specimens will have to show the effects of these impurities on the material properties. It will also have to be examined if they must be removed by vacuum arc remelting (VAR). Instabilities of the process caused by the evaporation of calcium can be reduced by carrying out the remelting operation under increased pressure of e.g. 10 bar.

[1] B. E. Paton et al., *Adv. Eng. Mater.* **1999**, *2*, 59.
[2] B. Friedrich, J. Hammerschmidt, *BHM* **2001**, *146*, 203.
[3] J. Hammerschmidt, *Schriftenreihe des IME Bd. 8*, Shaker Verlag, Aachen **2003**.
[4] J.-C. Stoephasius, B. Friedrich, J. Hammerschmidt, in: *Ti-2003 Sci. and Technol.* Wiley-VCH-Verlag, Weinheim **2004**, 2209.
[5] J.-C. Stoephasius, B. Friedrich, in *Proc. Eur. Metall. Conf. 2005*, GDMB Medienverlag, Clausthal-Zellerfeld **2005**, 1429.
[6] F. Tsukihashi et al., *Metall. Mater. Trans.* **1996**, *27B*, 967.
[7] T. H. Okabe et al., *Mater. Trans. JIM* **1991**, *32*, 485.
[8] B.-J. Lee, N. Saunders, *Z. Metallkd.* **1997**, *2*, 152.
[9] R. O. Suzuki, S. Inoue, *Metall. Mater. Trans.* **2003**, *34B*, 277.
[10] B. D. Lichter, in *Landolt-Börnstein – Group IV*, Vol. 5C, Springer-Verlag, Heidelberg **1993**.
[11] L.-I. Staffansson, D. Sichem, *Scand. J. Metall.* **1992**, *21*, 165.
[12] A. I. Zaitsev, B. M. Mogutnov, *Metall. Mater. Trans.* **2001**, *32B*, 305.
[13] W. G. Seo et al., in *VII Int. Conf. on Molten Slags Fluxes and Salts* , Johannesburg **2004**, 835.
[14] M. G. Benz, W. T. Carter, in *4th Symp. Adv. Techn. and Proc. for Metals and Alloys*, ALD Vacuum Technologies AG, Erlensee **1999**, 86.
[15] H. Scholz, et al., in *Ti-2003 Sci. and Technol.* Wiley-VCH-Verlag, Weinheim **2004**, 205.
[16] A. D. Ryabtsev, *Ph. D. Thesis*, The E. O. Paton Electric Welding Institute of the National Academy of Sciences of Ukraine, Kiev **2004**.
[17] A. D. Ryabtsev et al., in *Proc. 2005 Int. Symp. on Liquid Met. Proc. and Casting*, Santa Fe, New Mexico, USA **2005**, 249.
[18] A.-M. Alvarez et al., *Acta Mater.* **2004**, *52*, 4161.
[19] C. Q. Chen, et al., *Acta Mater.* **2004**, *52*, 3697.
[20] A. Takasaki, Y. Furuya, *NanoStruct. Mater.* **1999**, *11*, 1205.

REVIEWS

ESR Refining Potential for Titanium Alloys using a CaF2-based Active Slag

*J.-C. Stoephasius, J. Reitz, B. Friedrich**

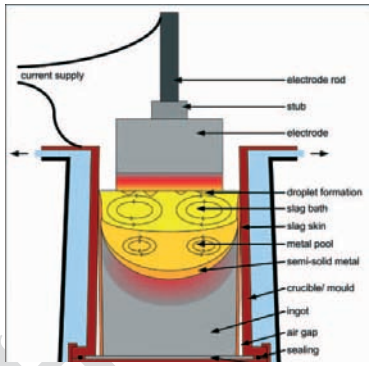

Since the end of the Cold War and due to the needs to produce titanium more cost-efficiently and thus more attractive for its civil use, the electroslag remelting (ESR) process has become an increasingly important topic of international research programs, because titanium and titanium aluminides can be chemically refined by ESR in some degree. Using ESR, titanium turnings from machining steps and scrap from foundries can be remelted, refined and provided as secondary titanium for the market at relatively favourable prices. This article investigates the removability of the main impurities out of titanium and titanium-aluminium alloys by electroslag remelting using the active slag system CaF_2-Ca-(CaO). Thermochemical and kinetic aspects of the ESR process are considered.

ADV. ENG. MATER. 2007, 9 ..... ■ ... ■

